COMMISSIONS 27 AND 42 OF THE IAU
INFORMATION BULLETIN ON VARIABLE STARS

Number 5398

Konkoly Observatory
Budapest
29 March 2003

HU ISSN 0374 – 0676

VV Cep OUTSIDE ECLIPSE

POLLMANN, E.

email: ErnstPollmann@aol.com

The 1997-1999 eclipse of the binary VV Cep gave researchers further opportunities to analyze the system. Bauer, Bennett and Brown (1998) attributed strong, double-peaked emission lines such as Mg II and Fe II in the ultraviolet range 2700-3000 Angstroms to an expanding atmosphere. They also reported that the hot B star was, during one orbital period, shrouded in a rich absorption spectrum of singly ionized elements. According to Leedjärv, Graczyk, Mikolajewski and Puss (1999) the eclipse occurred 68 days later than predicted which may indicate an orbital period change due to mass transfer between the M and B stars. Further, they suggested that the cooler object may be an asymptotic giant branch star instead of a supergiant. Graczyk, Mikolajewski and Janowski (1999) came to the same conclusion. They found masses for the M and B stars of about 2.5 and 8 solar masses, respectively, with a total mass ejection of 0.008 solar mass and a loss rate of 4×10^{-4} solar mass per year.

In an earlier paper (Pollmann, 2001) I presented observations of Hα emission strength in VV Cep, as measured in equivalent width (EW), from JD 2450202 to 2452061. The rate of sampling was high enough to reveal the eclipse in detail and to show asymmetric distribution of Hα intensity across the accretion disk as determined at the times of ingress and egress.

In this paper I report on continued observations in the period JD 2452061 to 2452619. I used the 200 mm Schmidt-Cassegrain telescope at the Cologne Stargazer's Association Observatory in the mountains of Odenthal, Germany (latitude: 51°02′, longitude: 7°15′). My spectrograph with diffraction grating has a dispersion of 0.39Å/pixel and a wavelength range of 6400Å to 6700Å. The detector is a Kodak KAF400 sensor with 768×512 pixels. Pixels are 9×9 micrometers. The resolving power is R = 8200. Data after JD 2451852 and discussed by Pollmann (2001) have also been observed with this instrument. Current results reveal apparent stochastic variation in Hα EW with a range of about 10Å outside eclipse. Despite these dispersions the EW seems to have increased after the eclipse within the period represented here with an upward gradient of approximately 1 Å/200d. There is also variability on a timescale of many hundreds of days. In Figure 1 the latter is identified by a linear fit to post-eclipse observations. Table 1 collects the observations that is also available electronically at the IBVS website as 5398-t1.txt. Exploration of both types of change is a likely project for the years leading up to the next eclipse that begins in 2017.

Wright (1977) observed Hα emission out of eclipse between 1956 and 1976. I determined V/R ratios from his Figure 4 plots and show them in Figure 2 along with my V/R results. Wright observed nearly an entire orbit with relatively few observations, while I was limited to phases from 0.14 to 0.24 with relatively more observations starting from JD 2451852. Prior to this date the resolution of the observed spectra did not allow to obtain V/R ratios. Figure 2 shows a phase-related cycle of change in V/R. In the short but significant range in which we overlap, my results agree with the pattern of rapid decrease detected by Wright. Erratic, short-term change in V/R is also indicated. Line profiles for my first and last observations appear in Figure 3. Table 2 presents all the V/R observations. I continue to observe Hα emission in VV Cep and will report again in the future.

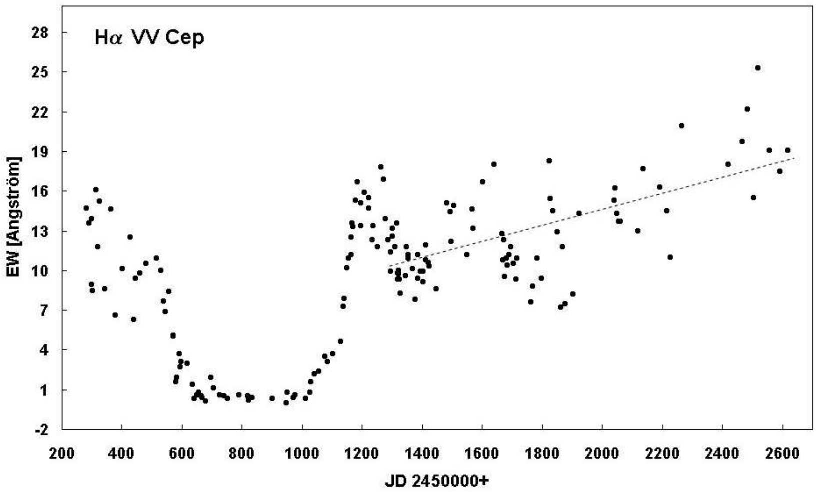

Figure 1. Hα equivalent width as a function of time for VV Cep before, during and after the 1997-1998 eclipse.

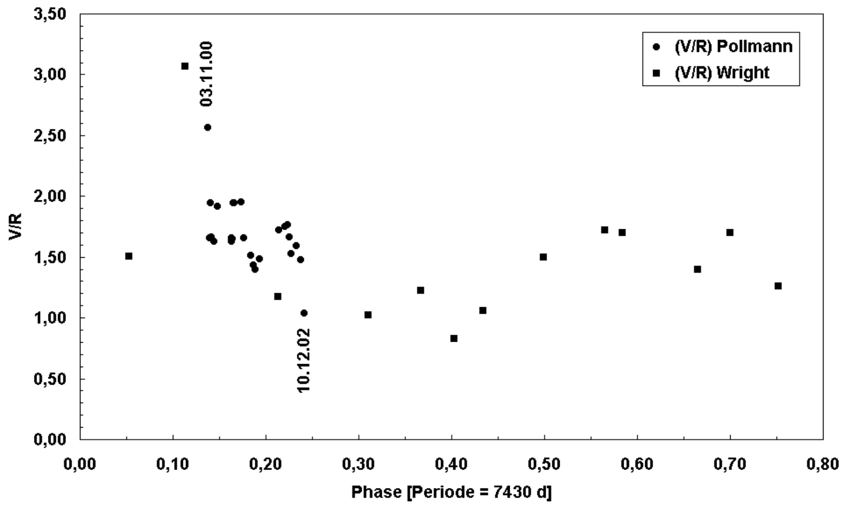

Figure 2. V/R ratio for the Hα emission line as a function of orbital phase as independently observed by Wright and Pollmann.

Table 1. Hα equivalent widths

JD 2450	EW [Å]	JD 2450	EW [Å]	JD 2450	EW [Å]	JD 2450	EW [Å]
282	14.7	752	0.3	1318	9.8	1685	10.4
291	13.6	790	0.6	1319	9.3	1690	11.2
298	13.9	819	0.5	1286	12.3	1696	11.8
299	8.9	823	0.2	1294	11.4	1703	10.5
301	8.5	835	0.4	1296	9.9	1712	9.3
313	16.1	902	0.3	1300	12.6	1716	10.9
321	11.8	949	0	1302	13.2	1447	8.6
327	15.2	952	0.8	1309	11.8	1762	7.6
343	8.6	970	0.4	1321	10	1769	8.8
363	14.6	976	0.6	1322	9.7	1782	10.9
379	6.6	1013	0.3	1324	9.3	1797	9.4
402	10.1	1027	0.8	1327	8.3	1825	18.3
428	12.5	1029	1.6	1345	9.6	1828	15.4
439	6.3	1040	2.2	1348	11.8	1835	14.5
444	9.4	1057	2.4	1353	11.2	1852	12.9
459	9.8	1077	3.5	1355	10.9	1863	7.2
480	10.5	1086	3.1	1376	7.8	1869	11.8
514	10.9	1102	3.7	1369	10.1	1877	7.5
529	10	1128	4.6	1385	11.2	1902	8.2
538	7.7	1137	7.3	1386	9.4	1924	14.3
546	6.9	1140	7.9	1395	9.9	2039	15.3
555	8.4	1150	10.2	1402	9.1	2042	16.2
570	5.1	1154	10.9	1403	9.9	2050	14.3
572	5	1164	11.2	1411	10.8	2055	13.7
581	1.6	1165	12.5	1413	11.9	2061	13.7
584	1.9	1168	13.6	1420	10.6	2120	13
592	3.7	1171	13.3	1424	10.3	2135	17.7
594	2.7	1178	15.3	1482	15.1	2191	16.3
597	3.1	1184	16.7	1495	14.4	2214	14.5
618	3	1196	13.4	1498	12.2	2228	11
635	1.4	1197	15.1	1505	14.9	2266	20.9
641	0.3	1208	15.9	1550	11.2	2420	18
649	0.6	1221	14.7	1567	14.6	2467	19.7
657	0.8	1222	15.5	1569	13.2	2485	22.2
664	0.5	1234	12.3	1601	16.7	2503	15.5
668	0.4	1237	13.4	1641	18	2519	25.3
679	0.1	1250	11.8	1665	12.8	2556	19.1
697	1.9	1263	17.8	1670	10.8	2593	17.5
704	1.1	1271	16.9	1671	12.3	2619	19.1
727	0.6	1278	13.9	1674	9.5		
741	0.5	1315	13.6	1681	10.9		

Table 2. Orbital Phase and Related V/R Ratios

JD	Phase	(V/R) Wright	JD	Phase	(V/R) Pollmann	JD	Phase	(V/R) Pollmann
2435572	0.053	1.504	2451852	0.138	2.563	2452191	0.184	1.510
2436810	0.113	3.067	2451863	0.139	1.655	2452214	0.187	1.433
2437554	0.214	1.174	2451869	0.140	1.941	2452228	0.189	1.395
2438272	0.310	1.019	2451877	0.141	1.662	2452266	0.194	1.481
2438694	0.367	1.222	2451902	0.145	1.625	2452420	0.214	1.723
2438960	0.403	0.828	2451924	0.148	1.919	2452467	0.221	1.750
2439189	0.434	1.059	2452039	0.163	1.659	2452485	0.223	1.764
2439675	0.499	1.501	2452042	0.164	1.631	2452503	0.226	1.665
2440165	0.565	1.720	2452050	0.165	1.650	2452519	0.228	1.530
2440304	0.584	1.699	2452055	0.165	1.944	2452556	0.233	1.592
2440908	0.665	1.400	2452061	0.166	1.944	2452593	0.238	1.479
2441166	0.700	1.700	2452120	0.174	1.950	2452619	0.241	1.034
2441555	0.752	1.263	2452135	0.176	1.660			

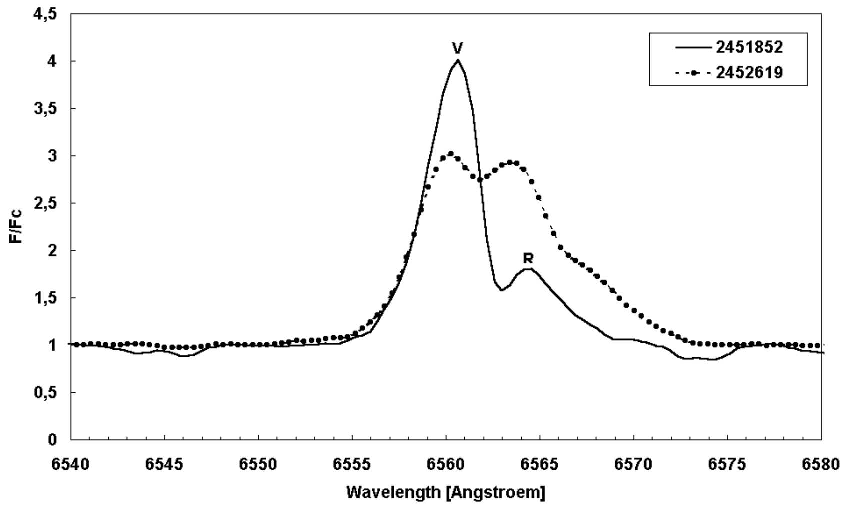

Figure 3. Hα emission line profiles at JD 2451852 and 2452619 as they appeared at phases 0.14 and 0.24, respectively.

References:

Bauer, W. H., Bennett, P. D., Brown, A., 1998, *BAAS*, **30**, 1319
Graczyk, D., Mikolajewski, M., Janowski, J. L., 1999, *IBVS*, No. 4679
Leedjärv, L., Graczyk, D., Mikolajewski, M., Puss, A., 1999, *A&A*, **349**, 511
Pollmann, E., 2001, *IBVS*, No. 5173
Wright, K. O., 1977, *JRASC*, **71**, 152